archives
of thermodynamics
Vol. **33**(2012), No. 2, 47–65
DOI: 10.2478/v10173-012-0010-3

Experimental investigation of the two-phase flow regimes and pressure drop in horizontal mini-size rectangular test section

AMR MOHAMED ELAZHARY*
HASSAN M. SOLIMAN

Department of Mechanical and Manufacturing Engineering, University of Manitoba, Winnipeg, Manitoba, Canada R3T 5V6

Abstract An experimental study was conducted in order to investigate two-phase flow regimes and fully developed pressure drop in a mini-size, horizontal rectangular channel. The test section was machined in the form of an impacting tee junction in an acrylic block (in order to facilitate visualization) with a rectangular cross-section of 1.87-mm height on 20-mm width on the inlet and outlet sides. Pressure drop measurement and flow regime identification were performed on all three sides of the junction. Air-water mixtures at 200 kPa (abs) and room temperature were used as the test fluids. Four flow regimes were identified visually: bubbly, plug, churn, and annular over the ranges of gas and liquid superficial velocities of $0.04 \leq J_G \leq 10$ m/s and $0.02 \leq J_L \leq 0.7$ m/s, respectively, and a flow regime map was developed. Accuracy of the pressure-measurement technique was validated with single-phase, laminar and turbulent, fully developed data. Two-phase experiments were conducted for eight different inlet conditions and various mass splits at the junction. Comparisons were conducted between the present data and former correlations for the fully developed two-phase pressure drop in rectangular channels with similar sizes. Wide deviations were found among these correlations, and the correlations that agreed best with the present data were identified.

Keywords: Mini channel; Two-phase; Flow regimes; Pressure drop

*Corresoponding author. E-mail address: umelazha@cc.umanitoba.ca

Nomenclature

C	–	coefficient used in Eq. (7)
C_1, C_2	–	coefficients used in Eq. (3)
D_H	–	hydraulic diameter, m
f	–	Fanning friction factor,
G	–	mass flux, kg $\mathrm{m}^{-2}\mathrm{s}^{-1}$
J	–	superficial velocity, ms^{-1}
$\dot{m}$	–	mass flow rate, $\mathrm{kg\,s}^{-1}$
p	–	pressure, Pa
p_r	–	reference pressure, Pa
Re_{D_H}	–	Reynolds number
X	–	parameter defined by Eq. (6)
x	–	quality
z	–	distance in the flow direction, m

Greek symbols

α	–	void fraction
μ	–	viscosity, $\mathrm{N\,s\,m}^{-2}$
ρ	–	density, $\mathrm{kg\,m}^{-3}$
ϕ	–	pressure-drop multiplier

Suscripts

1, 2, 3	–	sides 1, 2, and 3 of the tee junction
$Corr$	–	value predicted by a correlation
Exp	–	experimental value
G	–	gas
Hom	–	homogeneous
L	–	liquid
TP	–	two-phase value

1 Introduction

There has been a considerable interest recently in compact heat exchangers with mini- and microsized flow channels. These heat exchangers contain flow passages of various cross-sections (e.g., circular and rectangular), as well as various types of dividing tee junctions (e.g., branching and impacting). Therefore, a full understanding of the two-phase flow phenomena in minisize junctions and flow channels, including the flow regimes, the fully developed pressure drop in the channels, and the pressure drop and the phase separation at the junctions is essential for the proper design of minisize heat exchangers under conditions of boiling or condensation.

Several investigations have been reported on the fully developed flow regimes and pressure drop in mini-rectangular channels of various aspect

ratios (e.g., [1–9]). It had been noted in some of these investigations (e.g., [9]) that the flow regimes and pressure drop in narrow channels with large aspect ratios are strongly influenced by the height of the channel. While a large volume of research has been reported on two-phase flow in mini-channels, very little information is currently available on two-phase flow in mini-size tee junctions.

The objectives of this research project is to generate original experimental data, models, and correlations on two-phase flow in a minisize impacting tee junction with a rectangular cross-section. To the authors' best knowledge, this is the first study on mini-size impacting tee junctions in the literature. The results presented in this paper cover the first phase of this study, including the fully developed flow regimes and pressure drop in the three sides of the junction.

2 Experimental investigation

2.1 Test rig

A schematic diagram of the test rig used in the present study is shown in Fig. 1. Compressed air from the main line at an average pressure of 690 kPa (abs) was passed through a pressure regulator followed by a pressure controller in order to ensure a steady-state flow and also to have a fine control on the air pressure. The air was then passed through a filtration unit consisting of two filters; the first filter had a bore diameter of 1 μm and the second filter had a bore diameter of 0.01 μm. These two air filters were used to ensure clean air running through the test section. The air was then passed through a bank of flow meters (three rotameters with overlapping ranges) for measuring the air inlet flow rate before injection into the test section through the mixer. The distilled water used in the experiments was pumped into the loop using a programmed gear pump. Water leaving the pump was passed through a filtration unit consisting of two stages (one filter of a bore diameter 10 μm in stage **1** followed by four filters of a bore diameter 2 μm arranged in parallel in stage **2**). After the filtration unit, the water flow rate was measured using a bank of rotameters with overlapping ranges and then was introduced to the mixer. Downstream from the mixer, the two-phase mixture entered the inlet side of the junction, which consisted of a developing length and a fully developed length before reaching the junction. The pressure at the junction, for all the single-phase air and the two-phase experiments, was kept at 200 kPa (abs). The inlet two-

phase mixture was split at the junction into two outlet streams according to the desired mass split ratio. The air-water mixture in each of the outlet branches was directed to its respective separation tank, where the air and water were separated into two streams. The mass split ratio at the junction was controlled by adjusting the pressure in the two separation tanks. The pressure in each separation tank was set at the desired value by adjusting the air flow rate exiting the separation tank using a flow control valve. The air and water flow rates from each separation tank were each measured by a bank of rotameters with overlapping ranges. The air then was exhausted to the atmosphere and the water was returned back to the water reservoir to be reused.

Downstream from each air flow meter bank on the inlet and outlet sides of the tee junction, a pressure gauge and a thermocouple were installed to measure the local pressure and temperature. These measurements were required for calculating the air flow rate at each flow measurement station. On the water side, the temperature was measured at each flow meter bank in order to calculate the local density. The separation tanks had relief valves to ensure the pressure did not exceed a certain limit. Check valves were installed before the mixer on the water and air lines to prevent any backflow.

2.2 Test section

Top views of both the test section and the mixer are illustrated in Fig. 2. The whole test section was etched in an acrylic block with a surface area of 787.4 mm $\times$ 558.8 mm, and a thickness of 76.2 mm to facilitate flow visualization. The test section was in the shape of an impacting tee junction with a rectangular cross-sectional area of 20-mm width by 1.87 mm height. The pressure was measured at 22 locations in the inlet and the outlet sides. The locations of the pressure taps are shown in Fig. 2.

A developing length of 53 hydraulic diameters was used in the inlet side of the junction before the flow reached the first pressure tap. The pressure measurement in the inlet side was done in the fully developed length of 41 hydraulic diameters. Each of the two outlets of the junction was about 90 hydraulic diameters in length and included developing and fully developed regions. The mixer was designed to be a part of the test section. It consisted of a stainless-steel plate fixed in the beginning of the test section at the bottom of the channel. The bottom of the channel and the stainless steel plate had the same level to prevent any unnecessary disturbances in the flow. Twelve holes were drilled in the stainless steel plate to act as an air

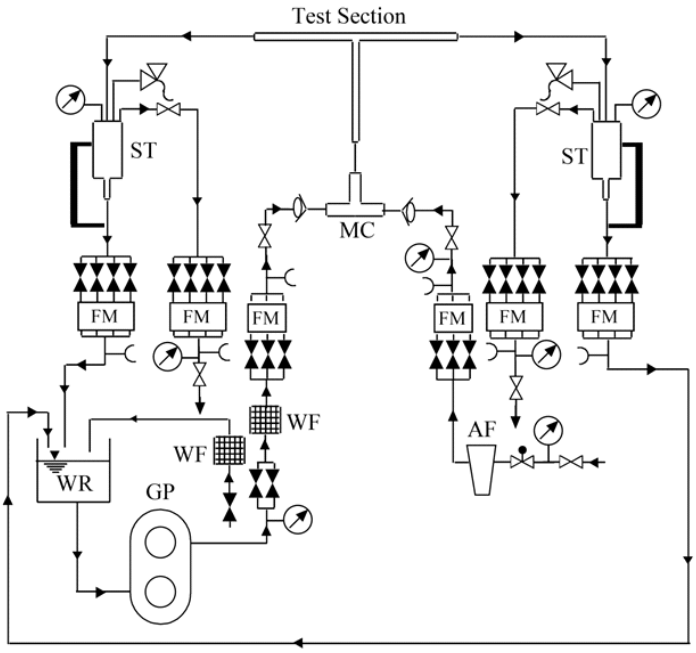

LEGEND

Symbol	Description	Symbol	Description
AF	Air Filter		Thermocouple
FM	Rotameter		Pressure Gauge
MC	Mixing Chamber		Check Valve
GP	Pump		Control Valve
ST	Separation Tanks		Pressure Controller
WR	Water Reservoir		Valve
WF	Water Filter		Safety Valve

Figure 1. Schematic diagram of the test rig.

inlet. Each of these holes had a diameter of 2 mm. A schematic diagram of the mixer is illustrated in Fig. 2.

2.3 Measuring devices

The air and water volume flow rates were measured using 22 rotameters. The air rotameters were calibrated using wet test meters and venturi me-

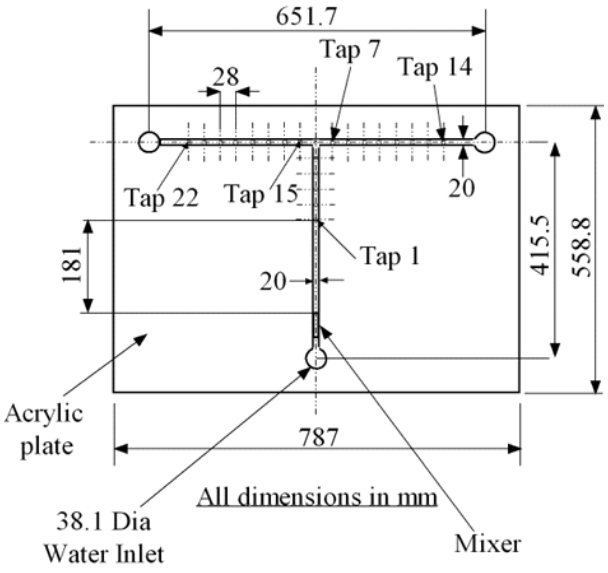

Test section

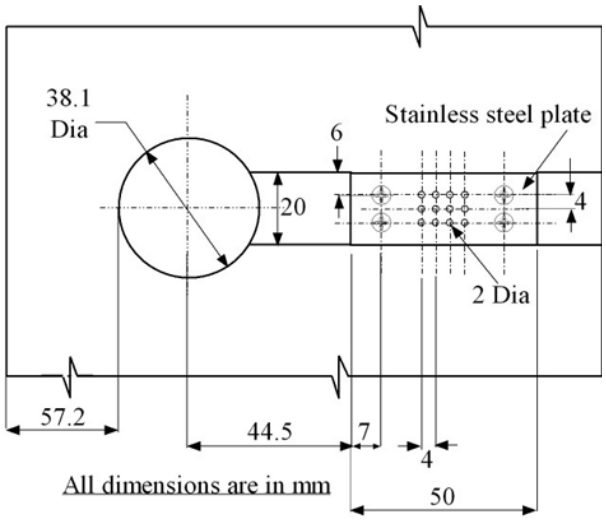

Top view of mixer

Figure 2. Details of the test section and the mixer.

ters, the calibration of which traces back to the National Institute of Standards and Technology (NIST), while the water rotameters were calibrated using a weigh and time method. Seven differential pressure transducers were used to measure the pressure distribution through the 22 taps in the test section. These transducers were calibrated using a micromanometer, a water manometer, and a mercury manometer depending on the transducer range. The pressure and temperature at different locations in the loop were measured using analog pressure gauges and thermocouples. The pressure gauges were calibrated using a deadweight tester and the thermocouples were calibrated at the ice point and boiling point against precession thermometers. A data acquisition system operated by the *LabView* software was used to collect and process the data from the pressure transducers and the thermocouples. The flow regimes were visualized and recorded using a digital camera.

The procedure of Kline and McClintock [10] was used to estimate the uncertainties in the measured and calculated variables. The resulting values are listed in Tab. 1.

Table 1. Experimental uncertainties.

Variable	Uncertainty range [%]
J_{L1}	$\pm 4.2 - \pm 6.7$
J_{G1}	$\pm 5.1 - \pm 9.8$
J_{L2}	$\pm 4.1 - \pm 7.0$
J_{G2}	$\pm 5.0 - \pm 6.8$
J_{L3}	$\pm 4.1 - \pm 8.9$
J_{G3}	$\pm 5.0 - \pm 8.9$
x_1	$\pm 2.1 - \pm 9.9$
$(dp/dz)_{TP}$	$\pm 0.1 - \pm 4.5$

3 Results and discussion

3.1 Single-phase flow pressure drop

A series of experiments was executed to measure the fully developed pressure drop during single-phase flow in the inlet and the two outlets of the test section. The results were compared with the single-phase classical equations

(for the laminar flow) and correlations (for the turbulent flow) in order to validate the creditability of the test rig, the test procedure, and the measuring devices. The experiments were executed using both air and water as test fluids. The measured friction factors in the laminar region were compared with the exact solution from Shah and London [11], and the friction factors in the turbulent region were compared with empirical correlation proposed by Sadatomi *et al.* [12].

The results of the measured single-phase friction factors and the comparison with the aforementioned equations and correlations are shown in Fig. 3 for air as the test fluid. The root mean square deviation between the measurements and classical equations and correlations was found to be 8.8%. These results also indicate that the critical Reynolds number for the transition from laminar to turbulent flow is close to 2000. The results in Fig. 3 confirm the adequacy of the test rig and the test procedure, as well as the accuracy of the measuring device.

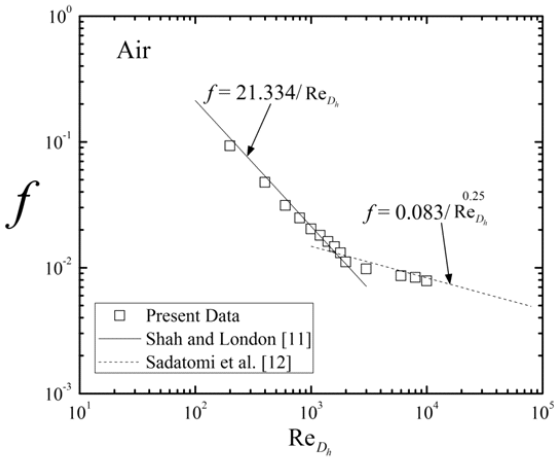

Figure 3. Single-phase air friction factor.

3.2 Flow regimes and their boundaries

A total of 116 experiments were performed to identify the flow regimes and establish the boundaries amongst them. The observed flow regimes corresponded to these ranges of superficial gas and liquid velocities: $0.04 \leq J_G \leq 10$ m/s and $0.02 \leq J_L \leq 0.7$ m/s, respectively. The flow regimes

were observed only in the fully developed region of the inlet side of the tee junction. fully developed conditions in this region were confirmed by the linear pressure drop during both single-phase and two-phase experiments. A digital camera was used to record the flow regimes. Based on the visual observations and the captured pictures, a flow regimes map was generated using the superficial gas and liquid velocities as coordinates. Four flow regimes were observed within the velocity ranges stated above. At a very small superficial gas velocity and high liquid superficial velocity, the bubbly flow regime was observed. Due to the small height of the test section, the spherical shape of the gas bubble deformed to a flattened shape. It was noticed that as the superficial liquid velocity increased, the gas bubbles broke down into smaller ones, as shown in Fig. 4a. The bubble break up is known to be caused by pressure forces resulting from turbulence in the liquid phase. At a smaller liquid velocity, the small gas bubbles agglomerated into larger ones due to bubble impacts at the lower liquid turbulence, as shown in Fig. 4b.

As the superficial gas velocity increased, flat elongated cylindrical shape gas bubbles formed in the test section with liquid bridging the gap between two consecutive bubbles. These bubbles had a plug-like shape, as shown in Fig. 4c. The length of the gas plugs increased as the superficial gas velocity increased; however, the length of the liquid bridge between the gas plugs did not significantly change by increasing the superficial gas and/or liquid velocities. This observation is consistent with the observation of Nicholson *et al.* [13] for macrosize channels.

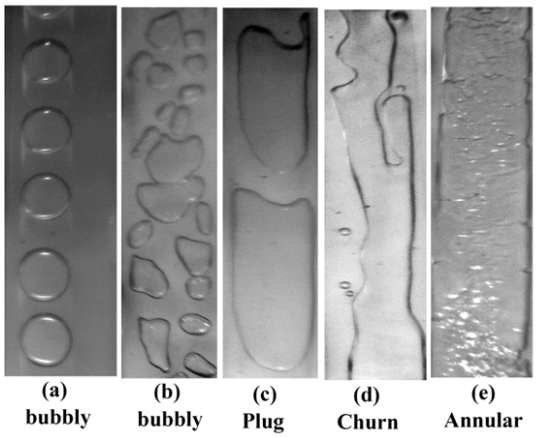

Figure 4. Photographs of observed flow regimes.

With a further increase of gas velocity, the liquid bridges between the gas plugs became unstable and the gas stream penetrated the liquid bridges forming a continuous gas core with liquid flowing along vertical walls of the channel. This flow regime, shown in Fig. 4d, is classified here as churn flow.

At high superficial gas velocities, the flow appeared as a gas core completely surrounded by a thin liquid film. It was not possible to determine by visual observation or digital photography whether liquid entrainment was present in the gas core or not. This flow regime, shown in Fig. 4e, was classified as annular flow. This flow regime is characterized by the domination of the inertia force even with the small size of the test section.

Ali et al. [14] reported that for narrow channels (e.g., 1.465 mm, which is close to the size of the present channel), the channel orientation from vertically upward to horizontal to vertically downward had a small effect on flow regimes and their transitions. Based on that observation, the generated flow regime map in this investigation for a horizontal channel was compared with two other flow regime maps developed for air-water flow in vertical channels. The first map was developed by Mishima *et al.* [7] for a test section with dimensions of 2.45 mm $\times$ 40 mm. The hydraulic diameter was 4.42 mm (35.2% larger than that of the present test section). The aspect ratio was 16.3 (52.3% larger than that of the present test section). The ranges of the superficial velocities were $0.01 \leq J_G \leq 100$ m/s and $0.1 \leq J_L \leq 10$ m/s. The second map was introduced by Ide *et al.* [3] for a test section with dimensions of 1.1 mm $\times$ 9.9 mm. The hydraulic diameter was 1.98 mm (42% smaller than that of the present test section). The aspect ratio was 9 (7.5% smaller than that of the present test section). The ranges of the superficial velocities were $0.5 \leq J_G \leq 20$ m/s and $0.1 \leq J_L \leq 0.7$ m/s.

Figures 5 and 6 show the above mentioned comparisons. The boundary between the bubbly and the plug flow regimes was not identified in the map introduced by Ide *et al.* [3] because their ranges of the superficial velocities did not cover the bubbly flow regime observed in the present study. The other flow regime boundaries given by Ide *et al.* [3] were closer to those of the present study than the regime boundaries given by Mishima *et al.* [7]. This observation indicates that the channel height could be more important in determining the boundaries between the flow regimes than the hydraulic diameter.

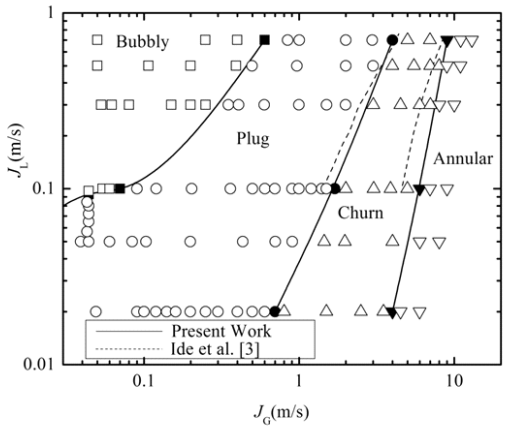

Figure 5. Comparison between the present flow regime map and the map of Ide *et al.* [3].

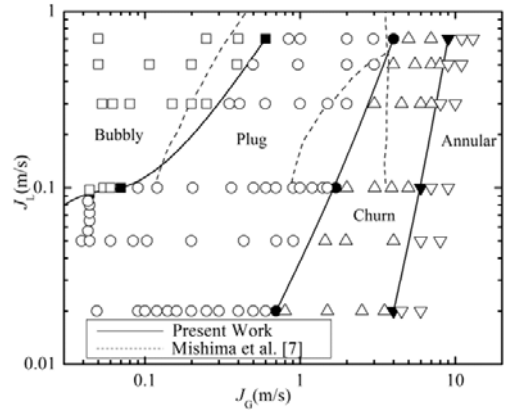

Figure 6. Comparison between the present flow regime map and the map of Mishima *et al.* [7].

3.3 Two-phase flow pressure drop

A sample of the pressure distribution measured on the three sides of the junction is shown in Fig. 7. Values of pressure, p, at all 22 taps were plotted relative to a reference pressure, p_r, which is the pressure at tap **1** (see Fig. 2). The fully developed pressure gradients on the three sides of the junction were determined by fitting linear equations to the fully developed data using the method of least-squares.

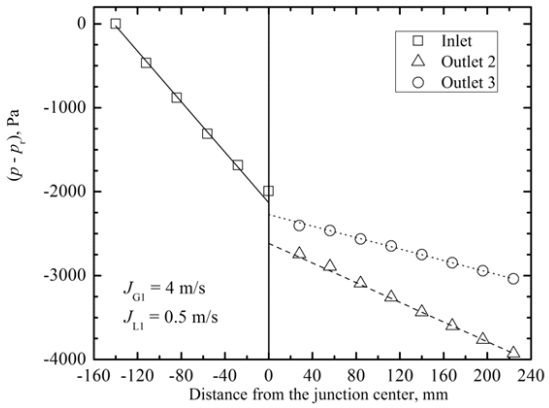

Figure 7. Sample of the measured pressure distribution.

The measured fully developed two-phase pressure gradients were compared with correlations from the literature. Some of those correlations were based on the homogeneous flow model (HFM) and the others were based on the separated flow model (SFM). The HFM is based on the assumption of equal velocity for the phases and therefore, the two-phase mixture is treated as a single-phase flow with averaged properties. Thus, the two-phase pressure gradient can be calculated from

$$(dp/dz)_{TP} = 2f\,G^2/(\rho_{Hom} D_H)\ , \tag{1}$$

where G is the mass flux, D_H is the hydraulic diameter, f is the friction factor, and ρ_{Hom} is the homogeneous density, given by,

$$\rho_{Hom} = (x/\rho_G + (1-x)/\rho_L)^{-1}\ , \tag{2}$$

where x is the mixture quality. The friction factor is usually given by

$$f = C_1 \mathrm{Re}_{D_H}^{C_2}\ , \tag{3}$$

where C_1 and C_2 are coefficients, and Re_{D_H} is Reynolds number expressed as

$$\mathrm{Re}_{D_H} = G\,D_H/\mu_{TP}\ , \tag{4}$$

where μ_{TP} is the equivalent viscosity of the two-phase mixture. For rectangular channels with the present aspect ratio, $C_1 = 21.334$ and $C_2 = -1$ in the case of laminar flow ($\mathrm{Re}_{D_H} \leq 2000$), while $C_1 = 0.083$ and $C_2 = -0.25$

in the case of turbulent flow ($\mathrm{Re}_{D_H} > 2000$). The difference among the HFM's reported in the literature is in the formulation of μ_{TP}.

Separated flow models (SFM) based on Lockhart and Martinelli [15] analysis are frequently used in correlating the two-phase frictional pressure gradient. The equations in this approach can be summarized by the following relations:

$$(dp/dz)_{TP} = \phi_L^2 \, (dp/dz)_L \ , \tag{5}$$

where ϕ_L is a two-phase pressure-drop multiplier, and $(dp/dz)_L$ is the frictional pressure drop if the liquid phase flows alone in the channel. Lockhart and Martinelli [15] correlated ϕ_L in terms of a parameter X defined as,

$$X^2 = (dp/dz)_L / (dp/dz)_G \ , \tag{6}$$

where $(dp/dz)_G$ is the frictional pressure drop if the gas phase flows alone in the channel. Lockhart and Martinelli showed that the variation of ϕ_L for a wide range of operating conditions is well represented by

$$\phi_L = 1 + \frac{C}{X} + \frac{1}{X^2} \ . \tag{7}$$

Several studies appeared in the literature in which the fully developed, two-phase, frictional pressure drop was correlated following the method given above by Eqs. (5)–(7). The main difference among these studies is in the formulation of the parameter C.

The present experimental results for the two-phase, fully developed, frictional pressure gradient were compared with 25 previous correlations from the literature and the results of these comparisons are listed in Tab. 2. The first seven entries in Tab. 2 correspond to the HFM given by Eqs. (1)–(4) with various formulations of μ_{TP}. The next 13 entries in Tab. 2 correspond to the SFM given by Eqs. (5)–(7) with various formulations of the parameter C in Eq. (7). The remaining five entries in Tab. 2 correspond to the SFM with formulations different from Eqs. (5)–(7). The deviations between the data and the correlations are quantified by the arithmetic mean deviation (AMD, %) and the root mean square deviation (RMSD, %). Table 2 shows large differences among the predictions obtained from different correlations. These large differences confirm that extreme care should be exercised when selecting a correlation for predicting $(dp/dz)_{TP}$ and that further research is required for developing correlations/models capable of more consistent predictions.

The best prediction among the seven HFM's in Tab. 2 was obtained from

the correlation of Beattie and Whalley [20] and the best prediction among the SFM's was obtained from the correlation of Zhang and Mishima [29]. These two comparisons are illustrated in Figs. 8 and 9, respectively.

Table 2. Summary of the comparison between the present data and existing correlations.

Author	AMD [%]	RMSD [%]
McAdams *et al.* [16]	1.3	29.5
Ackers *et al.* [17]	34.9	67.3
Cicchitti *et al.* [18]	125.7	200.2
Dukler *et al.* [19]	-34.8	41.0
Beattie and Whalley [20]	-6.7	20.9
Lin *et al.* [21]	42.9	75.6
Awad and Muzychka [22]	76.5	126.1
Chisholm [23]	-31.6	37.3
Wambsganss *et al.* [24]	-47.5	50.7
Mishima *et al.* [7]	28.6	49.9
Mishima and Hibiki [25]	40.9	61.2
Lee and Lee [6]	-43.0	47.9
Qu and Mudawar [26]	23.4	37.9
Lee and Mudawar [4]	25.9	35.4
Hwang and Kim [27]	-38.9	41.8
Zhang [28]	-22.7	27.4
Zhang and Mishima [29]	-10.7	28.8
Li and Wu [1]	45.9	78.5
Zhang *et al.* [30]	24.7	46.7
Tran *et al.* [31]	127.5	165.8
Friedel [32]	191.5	252.3
Müller-Steinhagen and Heck [33]	-3.7	38.1
Ide and Matsumura [8]	22.1	178.4
Ide *et al.* [3]	-26.3	34.7
Sun and Mishima [2]	17.9	40.8

The comparison shown in Fig. 8 indicates that the HFM can be successful in predicting the pressure gradient if the selected two-phase flow viscosity adequately reflected the characteristics of the flow regimes. Beattie and Whalley [20] started from the two-phase flow viscosity proposed by Dukler *et al.* [19] that is given by

$$\mu_{TP,\,Dukler} = \mu_G \alpha_{Hom} + \mu_L \left(1 - \alpha_{Hom}\right) \ , \tag{8}$$

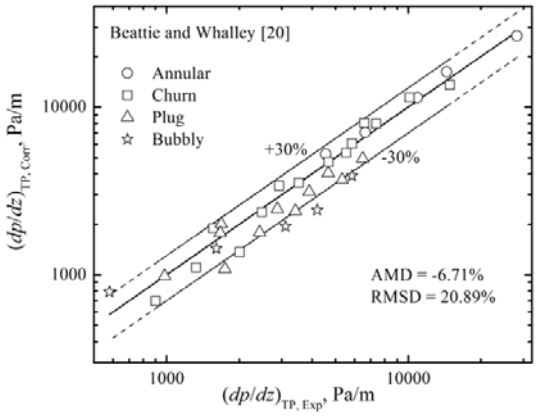

Figure 8. Comparison between the present data and the correlation due to Beattie and Whalley [20].

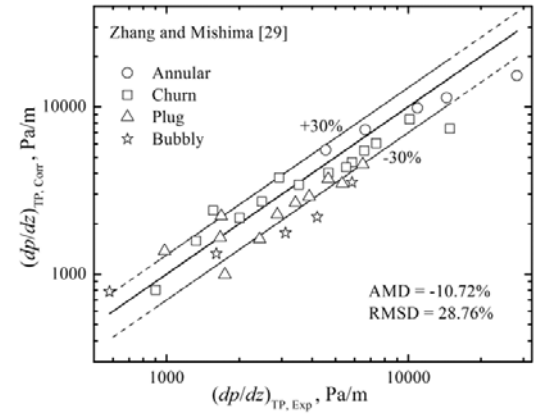

Figure 9. Comparison between the present data and the correlation due to Zhang and Mishima [29].

where the homogeneous void fraction is given by

$$\alpha_{Hom} = \frac{x\,(\rho_L/\rho_G)}{x\,(\rho_L/\rho_G) + (1-x)}\,. \tag{9}$$

Beattie and Walley [20] stated that the viscosity expression given by Eq. (8) is more appropriate for annular flow because it was based on the concept that, due to interfacial waves, the viscosity at the outer region of the vis-

cous sublayer intermittently changes between the liquid viscosity and the gas viscosity with the intermittency fraction being assumed to be the homogeneous void fraction. Consequently, the expression given by Eq. (8) was intended to approach the gas viscosity when the void fraction approaches one and the liquid viscosity when the void fraction approaches zero. Beattie and Whalley modified Eq. (8) by replacing the liquid viscosity by a proposed viscosity that can be used for the bubbly flow. The final expression for the two-phase viscosity took the form

$$\mu_{TP} = \mu_G \alpha_{Hom} + \mu_L \left(1 + 2.5\,\alpha_{Hom}\right)\left(1 - \alpha_{Hom}\right) \ . \tag{10}$$

Expression (10) still gives $\mu_{TP} \to \mu_L$ as $\alpha_{TP} \to 0$. As Fig. 8 suggests, the modification introduced by Beattie and Whalley [20] succeeded in producing good predictions for the four flow regimes observed in the present study.

The correlation proposed by Zhang and Mishima [29] was based on the SFM expressed by Eqs. (5)–(7). The coefficient C in Eq. (7) was based on a concept that was first proposed by Sugawara *et al.* [34]. Sugawara *et al.* conducted experiments on small-diameter tubes and observed that as the tube diameter decreased, the momentum coupling between the gas and liquid phases decreased and that was directly reflected on the value of the coefficient C. In other words, as the diameter of the tubes decreased, the value of the coefficient C decreased. Hypothetically, the coefficient C was suggested to be zero at a hydraulic diameter of zero. It was reported by Sugawara *et al.* that, at large hydraulic diameters, the coefficient C reached an asymptotic value of 21. Instead of correlating the parameter C in terms of the hydraulic diameter [34], Zhang and Mishima [29] correlated the coefficient C in terms of a confinement number to extend the validity of the correlation to different test fluids.

For the conditions covered in the present experiment, the coefficient C, as suggested by Zhang and Mishima [29], has a constant value of a 7.56 for the whole range. This value of C covers the range of laminar or turbulent gas flow and laminar liquid flow, which were the combinations encountered in the present experiment. The value of 7.56 is almost the average of the two values of the coefficient C suggested by Chisholm [23] for turbulent-laminar and laminar-laminar gas-liquid flows. As illustrated in Fig. 9, this choice of the parameter C gave satisfactory values of the AMD and the RMSD between the present data of all flow regimes and the correlation of Zhang and Mishima [29].

4 Conclusions

A research project dealing with two-phase flow in a mini-size horizontal impacting tee junction was initiated. The inlet and outlet sides of the junction had rectangular cross-sections with dimensions of 20 mm in the horizontal direction and 1.87 mm in the vertical direction. Air-water mixtures with 200 kPa (abs) at the junction were used as the test fluids. This paper reports results for the observed flow regimes in the three sides of the junction and the frictional, fully developed pressure gradient in the three sides of the junction measured during single- and two-phase flow tests. The following conclusions can be drawn from the results presented in this paper:

1. The measured single-phase pressure gradient deviated by a maximum of 8.8% from the exact solution (for laminar flow) and an empirical correlation developed for a similar aspect ratio (for turbulent flow). This agreement confirmed the credibility of the test rig, the accuracy of the measuring devices, and adequacy of the measuring technique.

2. Four flow regimes were observed: bubbly, plug, churn, and annular. Liquid only zones with a complete absence of gas existed in the bubbly flow regime at relatively low liquid superficial velocity and in the plug flow, which indicated the significant effect of surface tension.

3. Based on the comparisons between the present flow regime map and the maps generated by Ide *et al.* [3] and by Mishima *et al.* [7] for test sections of 1.1 mm × 9.9 mm and 2.45 mm × 40 mm, respectively, it is thought that the channel height could have a more significant role in determining the flow-regime boundaries than the hydraulic diameter.

4. The comparison between the present data of two-phase pressure gradient and 25 correlations from the literature resulted in wide deviations among the predictions from the different correlations. The best agreements with the present data were obtained with the HFM of Beattie and Whalley [20] and the SFM of Zhang and Mishima [29].

Acknowledgement The financial assistance provided by the Natural Sciences and Engineering Research Council of Canada is gratefully acknowledged.

Received 30 December 2011

References

[1] Li W., Wu Z.: *A general correlation for adiabatic two-phase pressure drop in micro/mini-channels*. Int. J. Heat Mass Transfer **53**(2010), 2732–2739.

[2] Sun L., Mishima K.: *Evaluation analysis of prediction methods for two-phase pressure drop in mini-channels*. Int. J. Multiphase Flow **34**(2009), 47–54.

[3] Ide H., Kariyasaki A., Fukano T.: *Fundamental data on the gas-liquid two-phase flow in minichannels*. Int. J. Therm. Sci. **46**(2007), 519–530.

[4] Lee J., Mudawar I.: *Two-phase flow in high-heat-flux micro-channel heat sink for refrigeration cooling applications: Part I-Pressure drop characteristics*. Int. J. Heat Mass transfer **48**(2005), 928–940.

[5] Kawahara A., Chung P., Kawaji M.: *Investigation of two-phase flow pattern, void fraction and pressure drop in microchannels*. Int. J. Multiphase Flow **28**(2002), 1411–1435.

[6] Lee H., Lee S.: *Pressure drop correlations for two-phase flow within horizontal rectangular channels with small heights*. Int. J. Multiphase Flow **27**(2001), 783–796.

[7] Mishima K., Hibiki T., Nishihara H.: *Some characteristics of gas-liquid flow in narrow rectangular ducts*. Int. J. Multiphase Flow **19**(1993), 115–124.

[8] Ide H., Matsumura H.: *Frictional pressure drops of two-phase gas-liquid flow in rectangular channels*. Exp. Therm. Fluid Sci. **3**(1990), 362–372.

[9] Troniewski L., Ulbrich R.: *Two-phase gas-liquid flow in rectangular channels*. Chem. Eng. Sci. **39**(1984), 751–765.

[10] Kline S., McClintock F.: *Describing uncertainties in single-sample experiments*. Mech. Eng. J. **75**(1953), 3–8.

[11] Shah R., London A.: *Laminar Flow Forced Convection in Ducts*. Academic Press, New York 1978.

[12] SadatomiI M., Sato Y., Saruwatari S.: *Two-phase flow in vertical noncircular channels*. Int. J. Multiphase Flow **8**(1982), 641–655.

[13] Nicholson M., Aziz K., Gregory G.: *Intermittent two phase flow in horizontal pipes: Predictive models*. Can. J. Chem. Eng. **56**(1978), 653–663.

[14] Ali M., Sadatomi M., Kawaji M.: *Adiabatic two-phase flow in narrow channels between two flat plates*. Can. J. Chem. Eng. **71**(1993), 657–666.

[15] Lockhart R., Martinelli R.: *Proposed correlation of data for isothermal two-phase, two-component flow in pipes*. Chem. Eng. Prog. **45**(1949), 39–48.

[16] McAdams, W., Woods W., Heroman L.: *Vaporization inside horizontal tubes of II-benzene-oil mixtures*. ASME Trans. **64**(1942), 193–200.

[17] Akers W., Deans H., Crosser O.: *Condensation heat transfer within horizontal tubes*. Chem. Eng. Prog. Symp. Series **55**(1959), 171–176.

[18] Cicchitti A., Lobaradi C., Silversti M., Soldaini G., Zavattarilli R.: *Two-phase cooling experiments – Pressure drop heat transfer burnout measurements*. Energia Nucleare **7**(1960), 407–425.

[19] Dukler A., Moye W., Cleveland R.: *Frictional pressure drop in two-phase flow Part A: A comparison of existing correlations for pressure loss and holdup, and Part B: An approach through similarity analysis*. AIChE J. **10**(1964), 38–51.

[20] Beattie D., Whalley P.: *Simple two-phase frictional pressure drop calculation method*. Int. J. Multiphase flow **8**(1982), 83–87.

[21] Lin S., Kwok C., Li R., Chen Z., Chen Z.: *Local frictional pressure drop during vaporization for R-12 through capillary tubes*. Int. J. Multiphase Flow **17**(1991), 95–102.

[22] Awad M., Muzychka Y.: *Effective property models for homogeneous two-phase flows*. Exp. Therm. Fluid Sci. **33**(2008), 106–113.

[23] Chisholm D.: *A theoretical basis for the Lockhart-Martinelli correlation for two-phase flow*. Int. J. Heat Mass Transfer **10**(1967), 1767–1778.

[24] Wambsganss M., Jendrzejczyk J., France D., Obot N.: *Frictional pressure gradients in two-hhase flow in a small horizontal rectangular channel*. Exp. Therm. Fluid Sci. **5**(1992), 40–56.

[25] Mishima K., Hibiki T.: *Some characteristics of air-water two-phase flow in small diameter vertical tubes*. Int. J. Multiphase Flow **22**(1996), 703–712.

[26] Qu W., Mudawar I.: *Measurements and predictions of pressure drop in two-phase micro-channel heat sinks*. Int. J. Heat Mass Transfer **46**(2003), 2737–2753.

[27] Hwang Y., Kim M.: *The pressure drop in microtubes and the correlation development*. Int. J. Heat Mass Transfer **49**(2006), 1804–1812.

[28] Zhang W.: *Study on constitutive equations for flow boiling in mini-channels*. PhD thesis, Kyoto University, 2006.

[29] Zhang W., Hibiki T., Mishima K.: *Correlation for flow boiling heat transfer at low liquid Reynolds number in small diameter channels*. J. Heat Transfer **127**(2005), 1214–1221.

[30] Zhang W., Hibiki T., Mishima K.: *Correlations of two-phase frictional pressure drop and void fraction in mini-channels*. Int. J. Heat Mass Transfer **53**(2010), 453–465.

[31] Tran T., Chyu M., Wambsganss M., France D.: *Two-phase pressure drop of refrigerants during flow boiling in small channels: An experimental investigation and correlation development*. Int. J. Multiphase Flow **26**(200), 1739–1754.

[32] Friedel L.: *Improved friction pressure drop correlation for horizontal and vertical two-phase pipe flow*. In: Proc. European Two-Phase Flow Group Meeting, Paper 2, 1979.

[33] Muller-Steinhagen H., Heck K.: *A simple friction pressure drop correlation for two-phase flow in pipes*. Chem. Eng. Process. **20**(1986), 297–308.

[34] Sugawara S., Katsuta K., Ishihara I., Muto T.: *Consideration on the pressure loss of two-phase flow in small-diameter tubes*. In: Proc. 4th National Heat Transfer Symp. of Japan, 169–172, 1967.